Title
MEASUREMENT OF POLARIZATION IN pi- p ELASTIC SCATTERING FROM 229 TO 3 90 MeV

Authors
Arens, John F.
Chamberlain, Owen
Dost, Helmut E.
et al.

Publication Date
2008-06-20

University of California

Ernest O. Lawrence Radiation Laboratory

MEASUREMENT OF POLARIZATION IN $\pi^- p$ ELASTIC SCATTERING FROM 229 TO 390 MeV

John F. Arens, Owen Chamberlain, Helmut E. Dost,
Michel J. Hansroul, Leland E. Holloway, Claiborne H. Johnson,
Claude H. Schultz, Gilbert Shapiro,
Herbert M. Steiner, and David M. Weldon

September 1967

Submitted to Physical Review

UCRL-17153 Rev.
Preprint

UNIVERSITY OF CALIFORNIA

Lawrence Radiation Laboratory
Berkeley, California

AEC Contract No. W-7405-eng-48

MEASUREMENT OF POLARIZATION IN π^-p ELASTIC SCATTERING FROM 229 TO 390 MeV

John F. Arens, Owen Chamberlain, Helmut E. Dost,
Michel J. Hansroul, Leland E. Holloway, Claiborne H. Johnson,
Claude H. Schultz, Gilbert Shapiro,
Herbert M. Steiner, and David M. Weldon

September 1967

MEASUREMENT OF POLARIZATION IN $\pi^- p$ ELASTIC SCATTERING FROM 229 to 390 Mev*

John F. Arens,[+] Owen Chamberlain, Helmut E. Dost,[++]
Michel J. Hansroul,[+++] Leland E. Holloway,[§] Claiborne H. Johnson
Claude H. Schultz,[§§] Gilbert Shapiro, Herbert M. Steiner, David M. Weldon[§§§]

September, 1967

ABSTRACT

The polarization parameter in elastic $\pi^- p$ scattering has been measured, at the Berkeley 184" synchrocyclotron, with the use of a polarized proton target. At 318, 337 and 390 Mev incident pion kinetic energy, the angular range from 70° to 180° in the center of mass system was covered. At 229 Mev polarization measurements were made in the angular range 150° to 180°. Phase shift analyses using these and other published data were made at the two lowest energies.

I. Introduction

The phenomenological analysis of low-to-medium energy pion-nucleon scattering has usually taken the form of phase-shift analyses.[1] This type of analysis has had the difficulty that, except at the lowest energies, it is not always possible to determine whether a unique solution exists.

A possible route out of this difficulty is to start with a well-established solution at a low energy and to continue this solution upwards at small increments in energy. At each energy one would make the requirement of any solution found that it not only fit the data well, but also that it join continuously to the (presumably unique) solutions found at lower energies. We do not exclude that other criteria such as those established by unitarity and causality considerations (i.e., dispersion relations) be also imposed. In this manner one may hope eventually to establish a phase-shift solution that is unique at all energies for which sufficient data exist.

The object of this experiment was to increase the amount of data available in order to try to pin down a unique solution at energies near ~300 Mev. At the same time we attempted to resolve certain inconsistencies among previously existing experiments[2,3] and analyses[4,5].

In the experiment reported here the polarization parameter, $P(\theta)$, in elastic $\pi^- p$ scattering was measured at incident pion kinetic energies of 318, 337 and 390 Mev, in the range from 70° to 180° in center-of-mass scattering angles. At 229 Mev, the angular range from 150° to 180° c.m.s. was covered. The technique used was single scattering from a polarized proton target. Scintillation counter hodoscopes were used to detect both final-state particles, with sufficient angular resolution to identify elastic scattering events from free protons. The measured asymmetry of the counting rate in any channel, upon reversal of the direction of target polarization (which is normal to the plane of scattering), can be directly related to the polarization parameter, $P(\theta)$, once the degree of polarization of the target is known.

Section II of this paper outlines the experimental procedure. Section III contains the results of this experiment. In section IV we present the results of a phase-shift analysis based on this and other results at 229 and 310 Mev.

II. Experimental Procedure

A. Beam and Target

The negative pion beams were produced at the internal target of the Berkeley 184" synchrocyclotron and guided out through the cyclotron shielding wall into a second shielded area known as the meson cave. The magnet system was designed so that it could be tuned to several different energies without having to move either the target or the concrete shielding. Momentum resolution was ±5%. Data were taken at beam kinetic energies centered at 229, 318, 337, and 390 Mev, as determined by range measurements, to within 2%.

The polarized target has been described elsewhere[6] and the principles of operation will not be repeated here.

Four crystals of $(.99\ La,\ .01\ Nd^{142})_2\ Mg_3\ (NO_3)_{12} : 24\ H_2O$, weighing a total of approximately 22 grams and filling a 1" diameter X 1" long cylinder, were used as the target. The hydrogen in the water of hydration provided the protons capable of being polarized by the method of dynamic nuclear orientation.

B. Method

The polarization parameter P in πN scattering was originally defined in terms of the recoiling nucleon from an unpolarized target. If the scattering is taken to be in the horizontal plane, then for a given center-of-mass angle θ,

$$P(\theta) = \frac{\text{number of nucleons with spin "up" minus number with spin "down"}}{\text{total number of nucleons recoiling at angle } \theta}$$

(This "up" direction is more precisely defined below as the direction $\hat{n}$.) Many such experiments have been performed, but they all have had to face the difficulty of determining the recoil polarization through making the nucleon scatter a second time.

With the assumption that parity is conserved in the interaction or that it is invariant under time reversal, however, the same parameter can be determined with only one scattering if that scattering is from a polarized target. Only the differential cross section $I(\theta)$ and target polarization $\vec{P}_T$ need be measured. The relation between P, I, and $\vec{P}_T$ is

$$I(\theta) = I_0(\theta)(1 + P(\theta)\hat{n}\cdot\vec{P}_T)$$

where I_0 is the differential cross section measured with an unpolarized target, and $\hat{n} = \hat{k}_i \times \hat{k}_f$ is the unit normal to the plan determined by the pion's initial and final momenta $\vec{k}_i$ and $\vec{k}_f$. In practice it is easier to avoid systematic errors by measuring the two rates I_+ and I_-, corresponding to scattering with target polarized in the direction of the normal to the plane of scattering and opposite to that normal, respectively. Then what is computed is the asymmetry

$$\epsilon(\theta) = \frac{I_+ - I_-}{I_+ + I_-}$$

Finally (ignoring background),

$$P(\theta) = \frac{\epsilon(\theta)}{P_T}$$

In the experiment reported here, $P(\theta)$ was determined by this second method. The target geometry was such that $\hat{n}$ and $\vec{P}_T$ were horizontal in the laboratory.

C. Counters and Electronics

All events were recorded as coincidences between two counter hodoscopes which detected the scattered pion and recoil proton as indicated in Fig. 1. To extend the available angular range without doubling the number of counters, the polarized target magnet was operated with opposite polarities at different times. In this way pions scattered at certain angle which would miss the array with one setting of the magnet will be deflected into the array with the opposite polarity. We hasten to point out that these polarity reversals are not required to reverse the direction of proton polarization. Target polarization reversal is accomplished, at either magnet polarity, by a change of 0.3% in the frequency of the microwave radiation used in the dynamic polarization process.

The pion hodoscope and the normal proton hodoscope each had 12 counters overlapped as shown in Fig. 1 to give 23 electronically distinguishable bins in the "θ" direction. The array used to detect protons when the magnet polarity was reversed used 11 such bins. In addition each array had 5 non-overlapping "φ" counters (not shown) running the full length of the arrays behind the θ counters. Anti-coincidence counters to left, right and above the beam were placed between the pole tips upstream from the crystal.

A coincidence between at least one counter in each of the four arrays (pion "θ", pion "φ", proton "θ", proton "φ") activated the "data-break" input channel to an on-line PDP-5 computer. The identities of all counters which had registered in coincidence were then stored directly in the computer memory later to be read out onto magnetic tape. The PDP-5 also performed a partial reduction of the data and displayed summaries of selected portions of it on an oscilloscope.

D. Data Analysis

Analysis of the IBM compatible data tapes produced by the PDP-5 was mainly performed using an IBM 7094 computer off-line. Events for which one and only one bin had registered in each array were further classified according to these bin numbers into a matrix having, typically, 23 X 5 X 23 X 5 = 13225 elements. This analysis was carried out separately for each beam energy and magnet polarity.

Elastic scatters from hydrogen in the target have well defined kinematics and form a narrow band through the matrix. Background events are more or less uniformly smeared over the whole matrix. A program which displayed graphically selected slices of the array was used to determine the hydrogen peak regions. The definition of these regions was then inserted into the final analysis program.

A dummy target, similar to the crystals with respect to quantity of the various atomic masses but containing no hydrogen, was used to measure the background due to scattering from heavy elements. Correction was also made for the presence of helium liquid in the vincinity of the target. The background from these sources was usually a small fraction of the counts in the channels corresponding to elastic scattering from hydrogen, in the worst cases amounting to 30% of the total in those channels.

The final computational program took the selected regions in the crystal and dummy target data and calculated the polarization parameter, $P(\theta)$, according to the following formulas:

$$P(\theta) = \frac{\epsilon}{1 - \bar{p}\,\epsilon}$$

where $$\epsilon = \frac{\sum_i N_i Q_i}{\left(\sum_i N_i - R \sum_j B_j\right) \overline{Q^2}}$$

i = i^{th} data taking run

N_i = number of counts (in hydrogen region, at scattering angle θ) during i^{th} polarized target run

j = j^{th} dummy target run

B_j = number of counts, in same region, during j^{th} dummy run

P_i = average target polarization during i^{th} run

m_i = number of monitor counts during i^{th} run

$$\bar{p} = \frac{\sum_i m_i P_i}{\sum_i m_i}$$ should be close to zero if data is evenly distributed between positive and negative target polarization.

$$Q_i = P_i - \bar{p}$$

$$\overline{Q^2} = \frac{\sum m_i Q_i^2}{\sum m_i}$$

$$R = \sum_i \sum_{NH} N_i \Big/ \sum_j \sum_{NH} B_j$$ (background is normalized to total counts in the non-hydrogen region)

NH refers to non-hydrogen regions of matrix.

Target polarization was reversed every two to three hours to keep possible long-term drifts from affecting data taken with one sign of target polarization differently than with the other.

The scattering angle was calculated using a computer program which found the trajectories of particles through the measured magnetic field. Conjugate proton and pion counters calculated in this fashion agreed perfectly with the hydrogen peak regions found in the data matrix. Within our resolution of about 1° laboratory angle, no evidence for error in scattering angle was formed.

E. Target Polarization Measurement

Target polarization was measured by a nuclear magnetic resonance technique, as described in references 6 and 7. This signal was monitored continuously during the run. Every half hour a slow (several minute) sweep through the NMR signal was made, during which the value of the rf level and its first derivative were digitized at small intervals. These data plus calibration signals (thermal equilibrium) which were taken approximately once every 24 hours were analyzed by computer program to give a corrected area under the resonance, which is thought to be proportional to the true polarization. The ratio of these areas, plus knowledge of the temperature and magnetic field at the crystal during calibration, yielded the absolute target polarization.

The polarization measured in this manner averaged 35% during this run. This rather low value may have been due to such factors as insufficient microwave power. On the other hand we cannot rule out the possibility of a systematic error in the polarization measurement. This possibility is supported both by internal evidence (certain difficulties encountered in the polarization-measuring electronics) and by external consistency with other data, mentioned below.

We assign a systematic error of ±10% to the calibration of the polarization measurement. This is to be interpreted as an uncertainty in the scale, to be applied uniformly to all the data reported in this article, in addition to the errors (largely statistical) reported here for the individual points.

III. Results

The results of this experiment are reported in Tables I, II, III and IV. They are presented graphically in Figures 2, 3, 4 and 5.

At 318 Mev, near where a conflict exists between measurements of Rugge and Vik[2] and those of Vasilevski et al.[3] at 310 Mev, our results tend to lie in between the two, but perhaps a bit closer to the former.

IV. Phase Shift Analysis

A. Input Data

Using the present polarization measurements along with other published data as input, we have made a phase-shift search at 229 and at 310 Mev.

The input data used, besides our own, were:

For 229 Mev: π^+p polarization at 246 Mev[8]; π^+p total and differential cross-section at 240 Mev[9]; π^-p total and differential cross-sections at 226 Mev[10]; and π^-p charge exchange differential cross-section at 230 Mev[11].

For 310 Mev: π^+p total and differential cross-sections at 310 Mev[12]; π^-p differential cross-section at 310 Mev[2]; π^-p charge exchange differential cross-section at 313 Mev[13]; π^+p polarization at 310 Mev[14]; and one point of $\pi^- p$ charge exchange polarization at 310 Mev[15].

A normalization parameter was introduced for each bloc of data to account for systematic uncertainties in the scale of each measurement. This parameter was allowed to vary in order to achieve the best fit. It was generally found that solutions found when the normalization parameters were held fixed at unity were not significantly different from those found when they were allowed to vary, but that they had considerably higher χ^2.

Also included were the non-spin-flip forward scattering amphitudes derived from dispersion relations.[16]

Partial wave amphitudes up to and including L = 3 (F- waves) were varied in the search for minimum χ^2, starting from values chosen randomly within certain regions described below.

Because of limited computer time and memory, it was considered impractical to generate the random starts from points selected uniformly throughout the total range of the variables (phase shift δ between -180° and $+180^\circ$; inelasticity parameter η between 0 and 1; for each partial wave). To reduce the region searched to manageable proportions we made use of the facts that: 1) the solutions should link up reasonably continuously with solutions found at nearby energies; 2) at these low energies, the elasticity is expected to be near unity; and 3) F- wave amplitudes are expected to be small. Whereas the starting points for the searches were selected within the restricted regions defined below, the solutions found proceeding from these starts were not so restricted.

The selected regions in each case centered about the solution found at a nearby energy by BBSV[4].

B. 229 Mev

At 229 Mev, the region for random starts was defined as follows: For S and P-waves, η between 0.9 and 1.0, δ within 45^o of the BBSV solution. For D-waves, η between 0.9 and 1.0, δ within 30^o of the BBSV solution. For F-waves $\eta = 1.0$, $\delta = 0^o$. Searches were made starting from 40 points chosen randomly within these limits.

The BBSV solution or minor modifications of this solution were found 16 times, with the confidence level of the best fit being 14%. Another solution of confidence level 8% was found once followed by solutions with confidence levels of 1% or less. Solution B can be excluded by using the Wigner condition[17] to link the 229 Mev phase shifts to the 310 Mev phase shifts given below. This condition states that $\frac{d\delta}{dk} \geqslant -R$ where R is the radius of interaction. Setting R equal to one pion Compton wave length, we find that the S_{31} phase shift either goes through an improbable resonance ($\delta = 90^o$) between 229 and 310 Mev or decreased 5 times more rapidly than the Wigner condition allows.

These two solutions are shown in Table V.

C. 310 Mev

At this energy an intensive search was made over a wide region of allowed starting points. 120 starts were made from a region which for S, P, and D waves allowed all values of η, from 0.0 to 1.0, and δ within 90^o (i.e,, a semi-circle) of the BBSV value. F-waves were started from

$\eta = 1.0$ and $\delta = 0^{\circ}$. No good solutions were found in any of these searches. 50 starts were made from a more restricted region, namely the same region defined above for the 229 Mev search, but with BBSV solutions appropriate to 310 Mev. Some acceptable solutions were now found. We conclude that in the previous case the search region was so wide that there was very small probability of finding a solution with χ^2 comparable to that of the BBSV solution.

40 starts were made from the same region, but with F-waves allowed to vary with the limits η between 0.95 and 1.0, δ between -10° and $+10^{\circ}$.

181 starts were made from regions centered at 0° phase shift, within the following limits: S_{11} and P_{11}, $\pm 30^{\circ}$; S_{31} and P_{31}, $\pm 90^{\circ}$; P_{13} and D_{13}, $\pm 23^{\circ}$; P_{33} and D_{33}, $\pm 45^{\circ}$; D_{15} and F_{15}, $\pm 19^{\circ}$; D_{35} and F_{35}, $\pm 38^{\circ}$; F_{17}, $\pm 15^{\circ}$; F_{37}, $\pm 30^{\circ}$. For S, P and D-waves, η between 0.9 and 1.0. For F-waves η between 0.95 and 1.0. These limits were selected so that any partial wave can by itself account for the known total cross-section. This procedure should be capable of finding every physically admissible solution.

The program was adjusted to find the minima with an accuracy of about one degree in the phase shifts δ and .01 in the elasticity parameters η; two minima as found by the computer were judged to be equivalent if they were identical to about this accuracy in every parameter. The BBSV solution was found[18] 14 times, with confidence level 37 percent. A similar, but not identical, solution was found

3 times; its confidence level was 6% and it had a rather different normalization factor for π^-p polarization than the first (BBSV) solution. Table VI shows the parameters for each of these solutions. Other solutions had confidence levels of 0.5% or less ($\chi^2 \geqslant 100$).

Table VII gives values of some quantities that were calculated from the various solutions. These quantities were not fit to experimental data within the program. The elastic cross-sections are reasonable in every case, but the inelastic cross-sections are generally too large. However, since very small changes in the η parameters would give agreement with the experimental numbers[19], it has seemed acceptable to leave the solutions as they are.

V. Conclusions

The results of this experiment demonstrate that:

With respect to the conflict in the π^-p polarization data[2,3] at 310 Mev, our results lie between the two, but tend to be closer to those of Rugge and Vik.

We confirm the solution of BBSV[4] as giving a good fit to all the data, including the results of the present experiment, which were not used in their original search.

The results of our phase shift search at 310 Mev seem to indicate that solution A is probably unique. Extensive searching throughout the region permitted by unitarity failed to discover any other solution with comparable χ^2. The slightly different solution B has marginally acceptable χ^2.

Further experiments have been undertaken at this laboratory to measure polarization in both π^+p and π^-p scattering in this energy range.

V. Acknowledgments

We wish to thank the crew of the 184" cyclotron, headed by J. Vale, and especially the accelerator technicians, under L. Silvia and R. Walton, as well as L. Wagner's counting group for valuable technical support.

Dr. P. Grannis composed the phase shift fitting programs used in this analysis.

FOOTNOTES AND REFERENCES

*This work was supported by the U. S. Atomic Energy Commission.

+Present address: Goddard Space Flight Center, N.A.S.A., Greenbelt, Maryland.

++Present address: Center for Naval Analyses, Arlington, Virginia.

+++Present address: Centre d'Etudes Nucleaires, Saclay, France.

§Present address: University of Illinois, Urbana, Illinois.

§§Present address: Columbia University, New York, New York.

§§§Present address: Los Alamos Scientific Laboratory, Los Alamos, New Mexico.

1. A. Barbaro-Galtieri, "Phenomenology of Resonances and Particles Supermultiplets, UCRL-17054, to be published in proceedings of School Ettore Majorana, Erice, Italy, 1966. These lectures contain references to most published πN phase shift analyses.
2. H. R. Rugge and O. T. Vik, Phys. Rev. 129, 2300 (1963).
3. I. M. Vasilevsky et al., Physics Letters 23, 174 (1966).
4. P. Bareyre, C. Brickman, A. V. Stirling, G. Villet, Physics Letters 18, 342 (1965). Hereafter referred to as BBSV. See also P. Bareyre, C. Brickman, G. Villet, submitted to Phys. Rev. (August, 1967).
5. P. Auvil and C. Lovelace, Nuovo Cimento 33, 473 (1964).
6. G. Shapiro, Progression Nuclear Techniques and Instrumentation 1, 176 (North-Holland, 1964). See also H. Atkinson in "Proceedings of the International Conference on Polarized Targets and Ion Sources" (Saclay, 1966) p. 41.
7. C. D. Jeffries "Dynamic Nuclear Orientation" (John Wiley, New York, 1963).

8. O. Chamberlain, C. D. Jeffries, C. H. Schultz, G. Shapiro, and L. Van Rossum, Phys. Letters 7, 293 (1963).

9. A. I. Mukhin, E. B. Ozerov, B. M. Pontecorvo, Zh. Eksperim. i Teor. Fig. 31, 371 (1956) English translation: Soviet Physics, JETP 4, 237 (1957) See also W. K. Troka et al., Phys. Rev. 144, 1115 (1966).

10. S. Kellmann, W. P. Kovacik, T. A. Romanowski, Phys. Rev. 129, 365 (1963).

11. J. C. Caris, R. W. Kenney, V. Perez-Mendez, W. A. Perkins III, Phys. Rev. 121, 893 (1961).

12. J. H. Foote, O. Chamberlain, E. H. Rogers, H. M. Steiner, Phys. Rev. 122, 959 (1961). See also P. M. Ogden et al., Phys. Rev. 137, B1115 (1965).

14. J. H. Foote, O. Chamberlain, E. H. Rogers, H. M. Steiner, C. E. Wiegand, T. Ypsilantis, Phys. Rev. 122, 948 (1961).

15. R. E. Hill, N. E. Booth, R. J. Esterling, D. L. Jenkins, N. H. Lipman, H. R. Rugge, O. T. Vik, Bull. Am. Phys. Soc. 9, 410 (1964).

16. J. Baacke, private communication. G. Hohler, G. Ebel, J. Giesecke, Zeit. F. Phys. 180, 430 (1964).

17. E. P. Wigner, Phys. Rev. 98, 145 (1955).

18. This solution agrees with that of Bareyre, Buciman, and Villet (August 1967) reference 4, to within one degree in 10 of 14 phase shifts and to within 2° in the remainder. The η's agree within .01 in 10 cases and within .02 in two more.

19. V. S. Barashenkov, V. M. Maltsev, Fortsch. Phys. 9, 549 (1961).

Table I. Experimental results for polarization in $\pi^- p$ scattering at 229 MeV. A systematic error of 10% is to be added because of uncertainty in the target polarization.

229 MeV		
θ_π^* (degrees, c.m.)	$P(\theta)$	$\Delta P(\theta)$
153.5	-.031	.051
155.9	-.030	.050
158.4	-.017	.046
160.8	-.063	.043
163.5	.054	.039
166.0	.102	.038
168.5	-.010	.040
171.1	.020	.036
173.8	.043	.035
176.3	..085	.037
178.6	.033	.058
178.9	..005	.043

Table II. Experimental results for polarization in π^-p scattering at 318 MeV. A systematic error of 10% is to be added because of uncertainty in the target polarization.

318 MeV		
θ^*_π (degrees c.m.)	$P(\theta)$	$\Delta P(\theta)$
66.8	-.892	.045
70.7	-.784	.036
74.6	-.654	.036
78.5	-.569	.035
82.3	-.501	.033
85.8	-.463	.035
89.3	-.310	.037
92.6	-.147	.042
96.1	-.113	.040
99.3	.070	.044
102.4	.165	.045
105.7	.292	.045
108.9	.332	.047
111.8	.524	.049
114.7	.529	.054
117.5	.523	.049
120.5	.668	.047
123.3	.530	.048
126.0	.529	.049
128.6	.489	.048
131.3	.511	.050
163.0	.280	.112
165.3	.207	.100
167.7	.164	.095
170.2	.134	.092
172.7	.120	.078
175.2	.028	.081
177.3	-.052	.101
177.7	-.007	.085
179.8	-.103	.087

Table III. Experimental results for polarization in π^-p scattering at 337 Mev. A systematic error of 10% is to be added because of uncertainty in the target polarization.

337 MeV		
θ_π^* (degrees c.m.)	$P(\theta)$	$\Delta P(\theta)$
73.5	-.709	.038
77.4	-.606	.039
81.2	-.619	.040
85.0	-.544	.037
88.5	-.363	.039
91.9	-.244	.047
95.2	-.190	.052
98.6	-.077	.055
101.8	.008	.053
104.9	.162	.057
108.1	.353	.061
111.2	.399	.052
114.1	.501	.061
116.9	.507	.060
119.8	.509	.060
122.7	.559	.055
125.4	.611	.053
128.1	.367	.064
130.7	.554	.057
133.4	.540	.063
161.6	.265	.071
164.2	.259	.060
166.5	.170	.053
168.9	.080	.049
171.4	.093	.044
173.9	.053	.042
176.1	.024	.058
176.4	.072	.041
178.6	-.031	.042
178.9	.118	.045

Table IV. Experimental results for polarization in π^-p scattering at 390 MeV. A systematic error of 10% is to be added because of uncertainty in the target polarization.

390 MeV		
θ_π^* (degrees, c.m.)	$P(\theta)$	$\Delta P(\theta)$
74.9	-.759	.036
78.8	-.716	.039
82.6	-.620	.042
86.4	-.610	.043
90.1	-.515	.047
93.5	-.353	.055
96.8	-.258	.057
100.0	.103	.070
103.3	.252	.078
106.5	.469	.066
109.5	.520	.079
112.6	.643	.079
115.6	.897	.074
118.5	.742	.074
121.2	1.020	.078
123.9	.821	.071
126.7	.728	.065
129.4	.796	.071
132.0	.688	.070
134.6	.692	.065
137.1	.524	.070
167.5	.119	.043
169.8	.112	.043
172.2	.054	.042
173.0	.059	.058
174.5	.113	.041
175.5	.000	.045
177.1	.049	.036
178.0	-.056	.038
179.5	.023	.037

Table V. 229 MeV. 18 degrees of freedom. δ in degrees. Phase shifts accurate to $\pm 1^{\circ}$. η's accurate to .01.

Solution		A	B
χ^2		25	27
S_{11}	η	1.00	1.00
	δ	10.2	6.2
P_{11}	η	1.00	1.00
	δ	4.4	2.3
P_{13}	η	1.00	1.00
	δ	-3.9	3.3
D_{13}	η	1.00	1.00
	δ	5.1	-5.6
D_{15}	η	1.00	1.00
	δ	-.6	5.5
F_{15}	η	.99	.97
	δ	3.1	-1.4
F_{17}	η	1.00	1.00
	δ	-1.4	.4
S_{31}	η	1.00	1.00
	δ	-16.6	74.7
P_{31}	η	.98	1.00
	δ	-4.9	-34.9
P_{33}	η	1.00	1.00
	δ	-64.9	-29.5
D_{33}	η	1.00	1.00
	δ	-2.2	-2.3
D_{35}	η	1.00	1.00
	δ	-.6	2.5
F_{35}	η	.97	1.00
	δ	-1.7	2.3
F_{37}	η	1.00	.97
	δ	3.4	-2.8
Normalizing factors for input data			
$\frac{d\sigma}{d\Omega}(\pi^+p)$		.99	1.00
		±.01	±.01
$\frac{d\sigma}{d\Omega}(\pi^-p)$		1.00	1.00
		±.01	±.01
$\frac{d\sigma}{d\Omega}$(ch.ex.)		.99	.99
		±.02	±.02
$P(\pi^+p)$		.96	.89
		±.01	±.08
$P(\pi^-p)$		.84	.84
		±.06	±.05

Table VI. 310 MeV. 66 degrees of freedom. δ in degrees. Phase shifts accurate to ±1°. η's accurate to .01.

Solution		A	B
χ^2		72.8	84.4
S_{11}	η	1.000	1.000
	δ	10.6	4.6
P_{11}	η	.97	.90
	δ	21.6	20.2
P_{13}	η	.96	.978
	δ	-4.6	-7.7
D_{13}	η	1.000	1.000
	δ	5.81	8.2
D_{15}	η	1.000	.982
	δ	.55	-.102
F_{15}	η	1.000	1.000
	δ	1.52	2.26
F_{17}	η	1.000	1.000
	δ	-.37	.21
S_{31}	η	.97	.964
	δ	-21.1	-32.4
P_{31}	η	.994	1.000
	δ	-10.8	-14.1
P_{33}	η	1.000	1.000
	δ	-41.3	-30.4
D_{33}	η	.957	.91
	δ	-2.1	-9.7
D_{35}	η	1.000	1.000
	δ	1.19	11.0
F_{35}	η	.980	.984
	δ	- .84	-.52
F_{37}	η	1.000	1.000
	δ	2.16	-1.07

Normalizing factors for input data.

	A	B
$\frac{d\sigma}{d\Omega}(\pi^+p)$	.91 ±.02	.89 ±.01
$\frac{d\sigma}{d\Omega}(\pi^-p)$	1.03 ±.02	1.00 ±.02
$\frac{d\sigma}{d\Omega}$(ch. ex.)	1.11 ±.04	1.07 ±.03
$P(\pi^+p)$	.99 ±.03	1.00 ±.03
$P(\pi^-p)$	.89 ±.03	.75 ±.03
P(ch.ex.)	1.03 ±.03	1.05 ±.03

TABLE VII. Values Calculated from Phase Shift Solutions

	Solution A	Solution B	Experiment[19]
<u>229 MeV</u>			
π^+ inelastic cross section	4.82 ± 1.50 mb	4.79 ± 1.15 mb	small
π^+ elastic cross section	125.63 ± 2.10 mb	126.82 ± 2.12 mb	σ_T = 130.00 ± 7.2 mb
π^- inelastic cross section	2.57 ± .65 mb	3.79 ± .69 mb	>0.3 ± 0.3 mb
π^- elastic cross section	16.05 ± .32 mb	16.00 ± .51 mb	20.8 ± 0.4 mb
charge exchange cross section	29.36 ± .65 mb	29.60 ± .68 mb	30.4 ± 1.3 mb
<u>310 MeV</u>			
π^+ inelastic cross section	4.78 ± .73 mb	6.96 ± .53 mb	small
π^+ elastic cross section	55.4 ± .8 mb	54.0 ± .6 mb	σ_T = 65.5 ± 1.7 mb
π^- inelastic cross section	3.57 ± .47 mb	5.77 ± .35 mb	1.47 ± .10 mb
π^- elastic cross section	10.47 ± .26 mb	10.51 ± .20 mb	11.4 ± 0.8 mb
charge exchange section	15.13 ± .27 mb	14.42 ± .19 mb	17.8 ± 1.0 mb

FIGURE CAPTIONS

Fig. 1. Polarized Target, Magnet and Scintillation Counter Arrays.

Fig. 2. Experimental results for polarization in π^-p scattering at 229 Mev. A systematic error of 10% in the vertical scale is to be added because of uncertainty in the target polarization.

Fig. 3. Experimental results for polarization in π^-p scattering at 318 Mev. A systematic error of 10% in the vertical scale is to be added because of uncertainty in the target polarization.

Fig. 4. Experimental results for polarization in π^-p scattering at 337 Mev. A systematic error of 10% in the vertical scale is to be added because of uncertainty in the target polarization.

Fig. 5. Experimental results for polarization in π^-p scattering at 390 Mev. A systematic error of 10% in the vertical scale is to be added because of uncertainty in the target polarization.

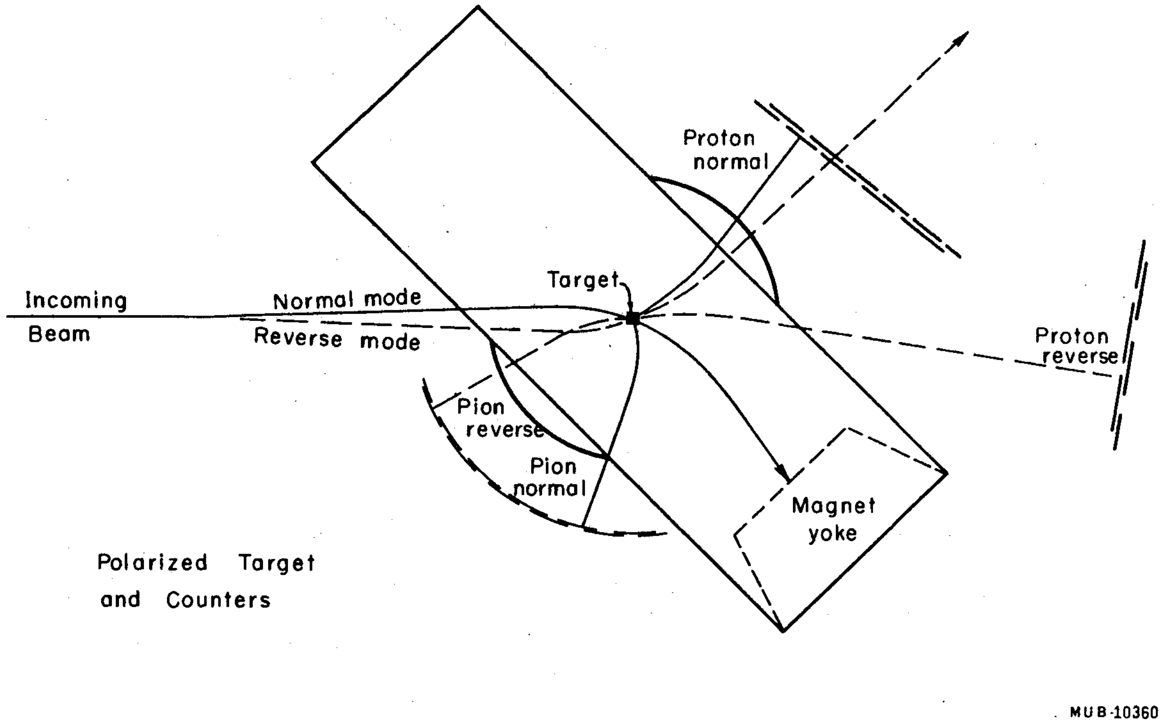
Proton
normal
Target
Incoming
Beam
Normal mode
Reverse mode
Proton
reverse
Pion
reverse
Pion
normal
Magnet
yoke
Polarized Target
and Counters
MUB-10360

Fig. 1

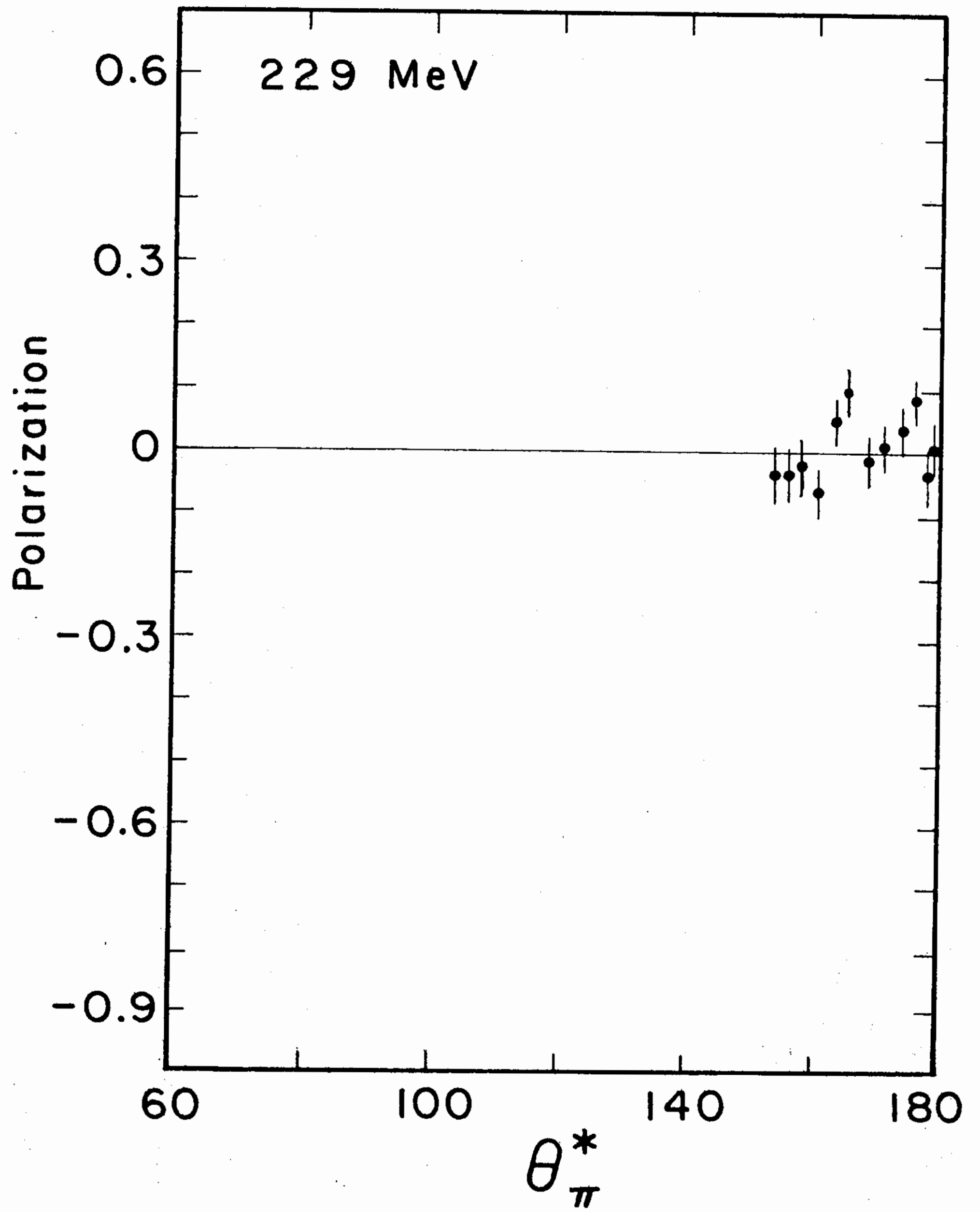
229 MeV
0.6
0.3
0
-0.3
-0.6
-0.9
Polarization
60
100
140
180
θ^*_π
MUB-12293

Fig. 2

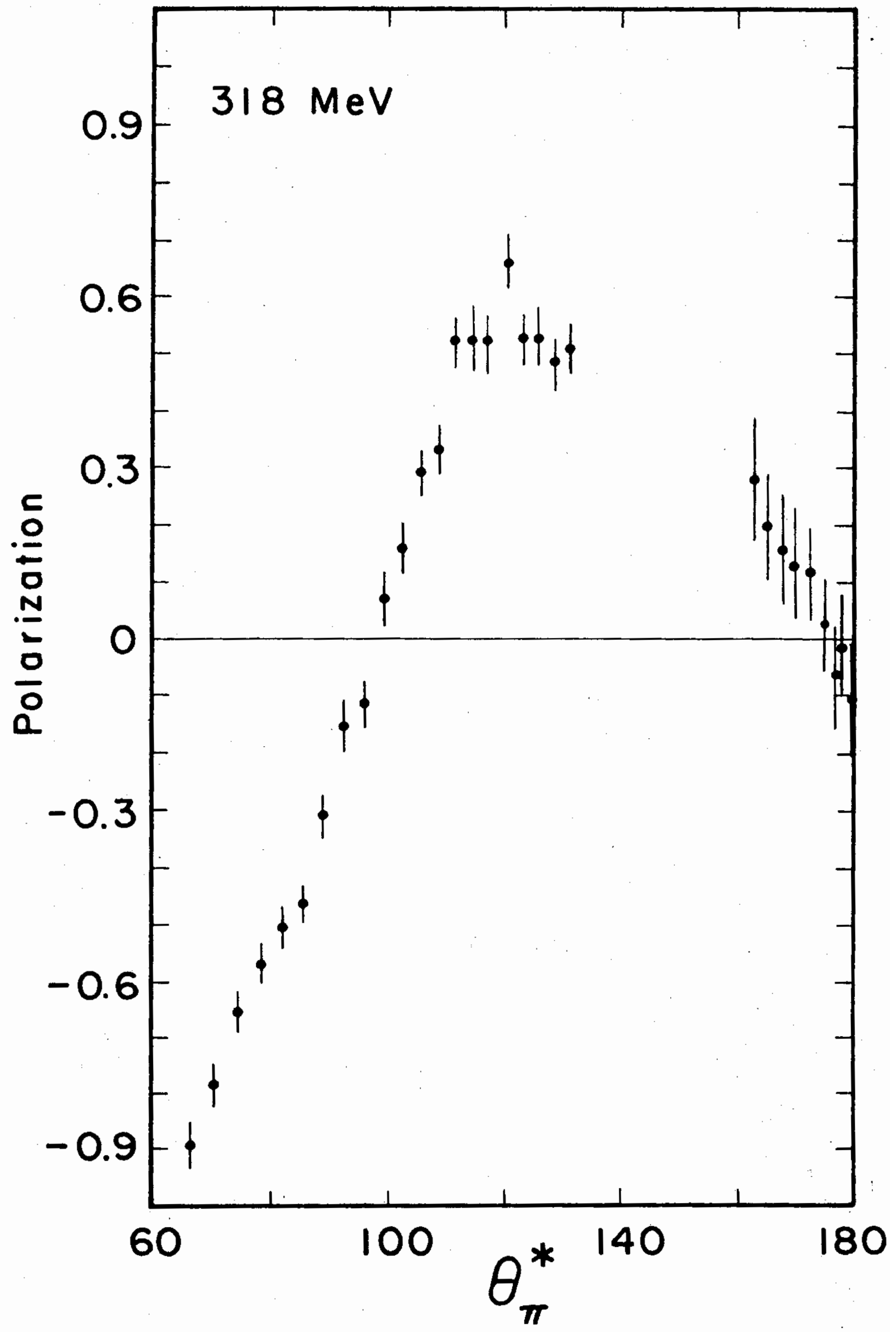

MUB-12295

Fig. 3

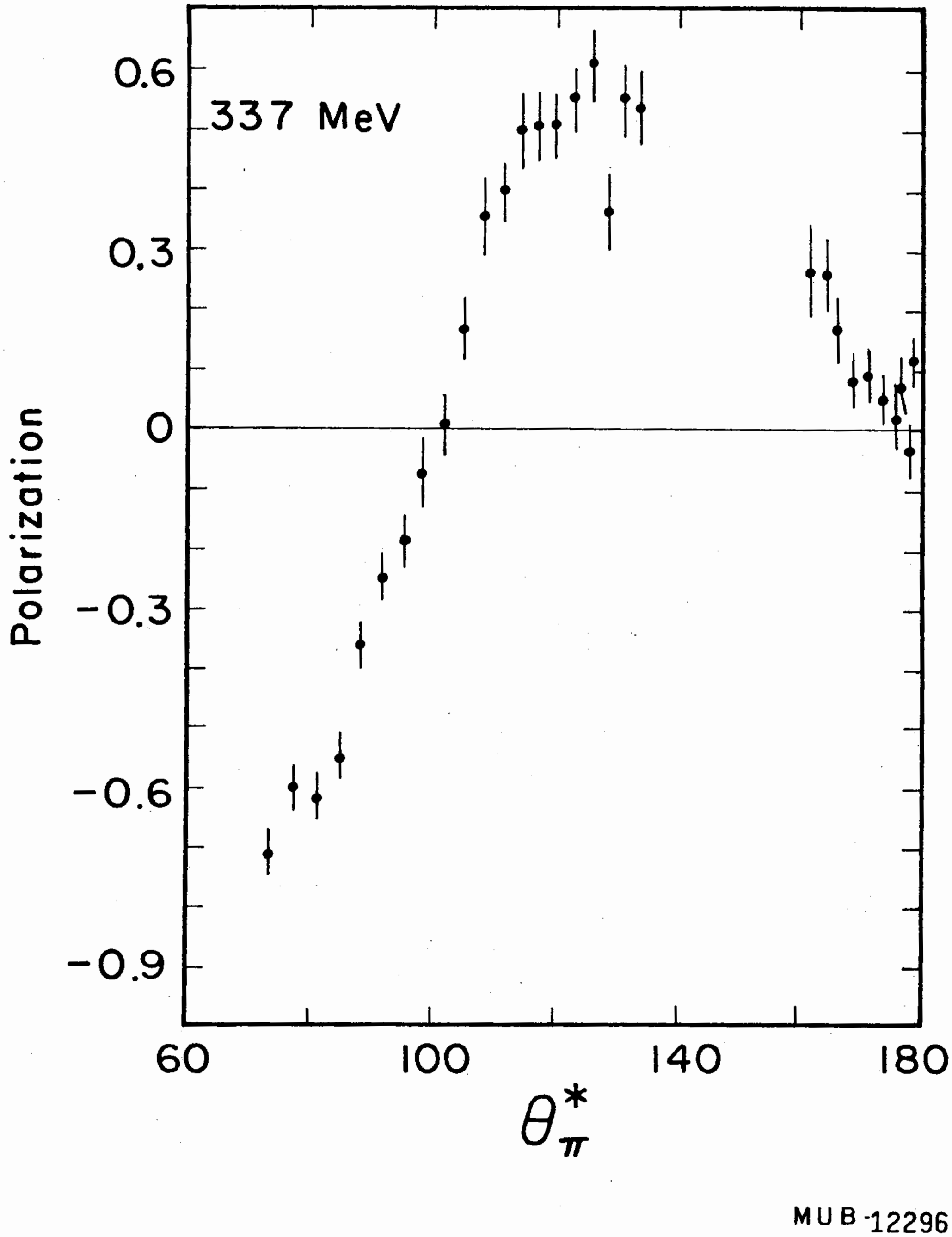
0.6
337 MeV
0.3
0
-0.3
-0.6
-0.9
Polarization
60
100
140
180
θ_π^*
MUB-12296

Fig. 4

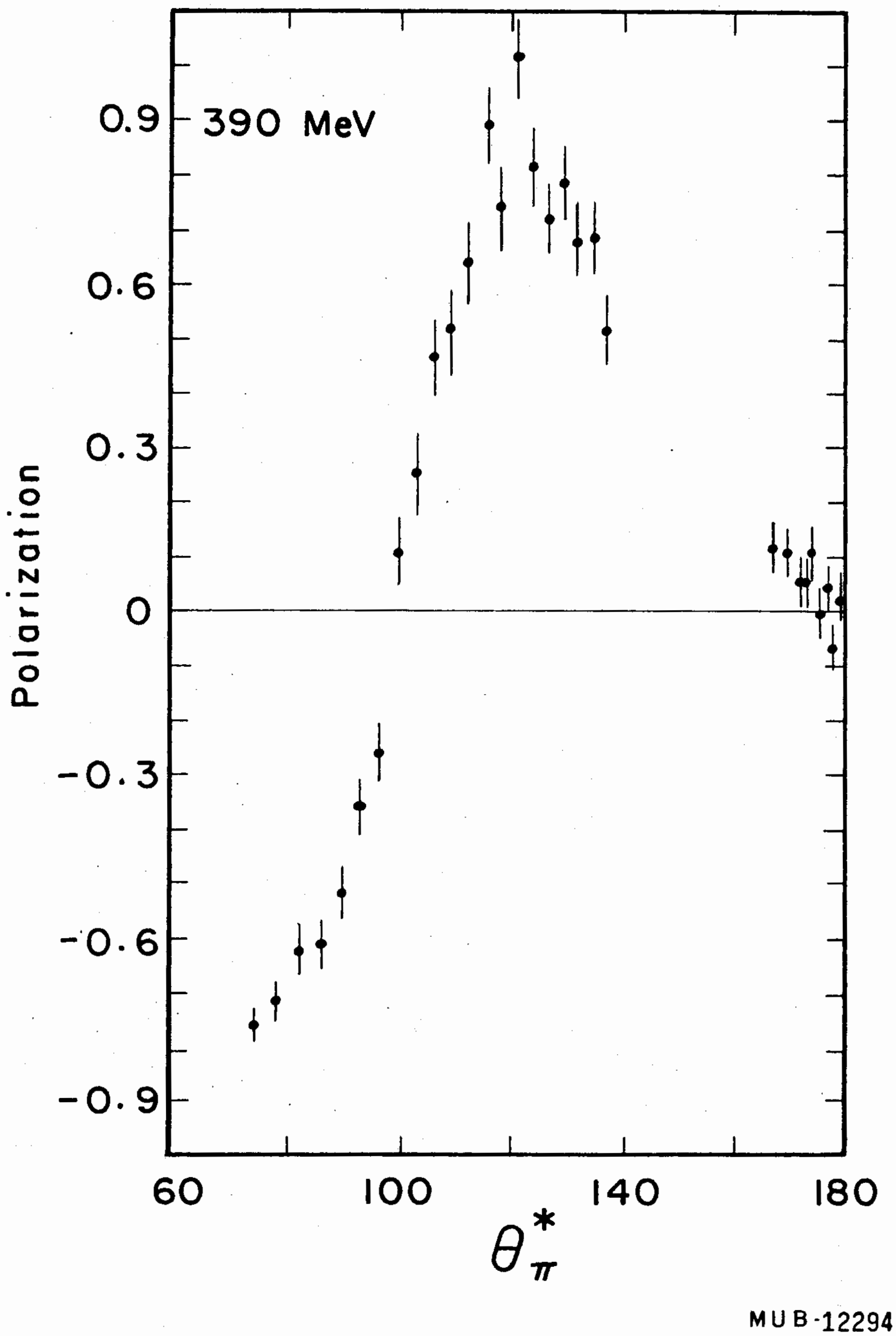

390 MeV
Polarization
0.9
0.6
0.3
0
-0.3
-0.6
-0.9
60
100
140
180
θ_{π}^{*}
MUB-12294

Fig. 5